

**Electrical signatures of ethanol-liquid mixtures: implications for monitoring biofuels migration in the subsurface**

Yves Robert Personna<sup>a\*</sup>, Lee Slater<sup>a</sup>, Dimitrios Ntarlagiannis<sup>a</sup>, Dale Werkema<sup>b</sup>, Zoltan Szabo<sup>c</sup>

*a. Department of Earth and Environmental Sciences, Rutgers University, 101 Warren Street, Newark, New Jersey, 07102 USA; [personna@pegasus.rutgers.edu](mailto:personna@pegasus.rutgers.edu) (Y.R. Personna),*

*[LSlater@andromeda.rutgers.edu](mailto:LSlater@andromeda.rutgers.edu) (L. Slater), [dimntar@andromeda.rutgers.edu](mailto:dimntar@andromeda.rutgers.edu) (D.*

*Ntarlagiannis)*

*b. U.S. EPA, NERL, ESD-LV, CMB, 944 E. Harmon Ave. Las Vegas, NV. 89119;*

*[Werkema.D@epamail.epa.gov](mailto:Werkema.D@epamail.epa.gov) (D. Werkema)*

*c. U.S. Geological Survey, New Jersey Water Science Center, 810 Bear Tavern Rd., Room 206, W.Trenton, New Jersey, 08628; [zszabo@usgs.gov](mailto:zszabo@usgs.gov) (Z. Szabo)*

\*Corresponding author e-mail: [personna@pegasus.rutgers.edu](mailto:personna@pegasus.rutgers.edu) (Y.R. Personna), Tel.: 973 353 5100, Fax: 973 353 1965

**ABSTRACT**

Ethanol (EtOH), an emerging contaminant with potential direct and indirect environmental effects, poses threats to water supplies when spilled in large volumes. A series of experiments was directed at understanding the electrical geophysical signatures arising from groundwater contamination by ethanol. Conductivity measurements were performed at the laboratory scale on EtOH-water mixtures (0 to 0.97 v/v EtOH) and EtOH-salt solution mixtures (0 to 0.99 v/v EtOH) with and without a sand matrix using a conductivity probe and a four- electrode electrical measurement over the low frequency range (1-1000 Hz). A Lichtenecker-Rother (L-R) type mixing model was used to simulate electrical conductivity as a function of EtOH concentration in the mixture. For all three experimental treatments increasing EtOH concentration resulted in a decrease in measured conductivity magnitude ( $|\sigma|$ ). The applied L-

R model fit the experimental data at concentration  $\leq 0.4\text{v/v}$  EtOH, presumably due to predominant and symmetric intermolecular (EtOH-water) interaction in the mixture. The deviation of the experimental  $|\sigma|$  data from the model prediction at higher EtOH concentrations may be associated with hydrophobic effects of EtOH-EtOH interactions in the mixture. The  $|\sigma|$  data presumably reflected changes in relative strength of the three types of interactions (water-water, EtOH-water, and EtOH-EtOH) occurring simultaneously in EtOH-water mixtures as the ratio of EtOH to water changed. No evidence of measurable polarization effects at the EtOH-water and EtOH-water-mineral interfaces over the investigated frequency range was found. Our results indicate the potential for using electrical measurements to characterize and monitor EtOH spills in the subsurface.

Key words: Geophysical methods; ethanol; biofuels; subsurface.

## **1. INTRODUCTION**

In the last two decades, the production of EtOH, one of the most common biofuels in the USA, has substantially increased due to regulations aimed at reducing air pollution and providing a supplement to petroleum. Accidental releases of large volumes of EtOH, particularly during transportation (Spalding et al, 2011) and at storage facilities (McDowell et al., 2003), have raised concerns about its environmental fate and potential risks to groundwater (Powers et al, 2001a). Ethanol is currently treated as an emerging contaminant (Gomez and Alvarez, 2010) that may induce substantial adverse effects in the subsurface environment (EPA, 2011). As a powerful disinfectant that has been long used as an antiseptic, EtOH at concentrations as low as 6% v/v is toxic to soil and aquifer microorganisms (Nelson et al, 2010). Ethanol toxicity can lead to major alterations in microbial growth, metabolism, viability (Ingram L.O., 1990; Nelson et al., 2010) and community structure (Cápiro et al., 2008; Ma et al., 2011). The persistence of EtOH toxicity in the subsurface may ultimately

lead to a substantial decrease in microbial population and activity, thus affecting the overall subsurface microbial processes including biodegradation of contaminants.

Ethanol contamination may also result in secondary adverse impacts on water quality. It has been shown that high EtOH concentration in water can exert cosolvency effects on existing BTEX (benzene, toluene, ethyl-benzene and xylene) contaminants (Powers et al., 2001b; DaSilva et al., 2002; Corseuil et al., 2004; Stafford et al., 2009). Ethanol is an amphiphilic molecule that is fully miscible in water. Ethanol is characterized by (1) a hydrophilic part (hydroxyl) allowing it to partition into water, and (2) a hydrophobic part (2-carbon alkyl chain) facilitating the remobilization and redistribution of organic compounds in the aqueous phase. Therefore, a high aqueous EtOH concentration can potentially lead to an enhancement of organic contaminant concentration in water (Powers et al., 2001b). Ethanol can also affect the natural degradation of BTEX compounds (Corseuil et al., 1998; Powers et al., 2001b; Ruiz-Aguilar et al., 2003; MacKay et al., 2006; Gomez and Alvarez, 2009 & 2010; Freitas et al., 2011a) due mainly to its preferential biodegradation and subsequent depletion of dissolved oxygen and other electron acceptors during this process, thereby limiting the degradation of the other compounds. As anaerobic conditions develop, EtOH degradation may generate methane in potentially hazardous concentrations by exceeding the explosive limit (Nelson et al., 2010; Freitas et al., 2010, Spalding et al., 2011).

Ethanol and water chemically form a complex mixture, which can be mainly attributed to the amphiphilic or bi-functional nature of ethanol molecules. These molecules are characterized by the hydrophilic hydroxyl group favorable to hydrogen-bonding formation with water molecules and the alkyl chain conferring hydrophobic effects (Franks and Ives, 1966). The complexity of EtOH-water media, partially attributable to the hydrogen-bond formation among the water and ethanol molecules, leads to complex molecular interactions (Atamas and

Atamas, 2009; Mizuno et al, 1995) and distinct physical properties of the solution (e.g. density and sound velocity) (Petek et al., 2001; Parke Birch, 1999) as the EtOH/water ratio changes.

Few studies have examined the potential of non-invasive geophysical measurements for monitoring the effects of EtOH releases in the subsurface environment. McNaughton et al. (2009) demonstrated the potential of using high frequency ground penetrating radar (GPR) to image sequential gasoline-EtOH releases in the near sub-surface. Petong et al. (2000) studied the dielectric relaxation of EtOH-water mixtures at different compositions and temperatures between 1 MHz and 24 GHz. At the low frequencies ( $< 1$  KHz) used for electrical conductivity and induced polarization methods, only Henderson et al. (2009) reported initial results that suggested the potential application of electrical measurements for EtOH detection in the subsurface.

Owing to the increasing likelihood of undesired EtOH releases, potential risks to humans and the environment exist, particularly in a scenario of a large EtOH spill and contamination of drinking water supplies. Such risks call for the preparation of adequate remediation responses. Yet, the design and application of relevant remediation actions depend both upon a comprehensive understanding of EtOH-water chemistry and the availability of cost-effective tools to characterize and monitor the spatial and temporal evolution of EtOH in the near surface. Therefore, basic research on the electrical properties of EtOH in water and porous media is needed in order to improve the understanding of the potential for electrical monitoring of ethanol contamination in the subsurface. In this paper, we investigate the low frequency ( $< 1$  KHz) geophysical behavior of EtOH-liquid (water and salt solution) mixtures at the laboratory scale. The main objective of this study was to determine the low-frequency electrical properties of EtOH in water and a porous medium. Our results indicate the

dependence of electrical conductivity measurements on EtOH concentration, highlighting the potential of electrical measurements for detection and monitoring of EtOH in the subsurface.

## 2. ELECTRICAL PROPERTIES

When applying an electrical current to a porous medium, electric conduction can occur as a result of electrolytic conduction through interconnected pores, electronic conduction in the presence of metals, and surface conduction in the electrical double layer (EDL) at the grain fluid interface. The electrolytic conductivity is controlled by the conductivity of the pore-filling electrolyte ( $\sigma_w$ ), along with the size and interconnectedness of the pores. The electronic conductivity occurs mainly as a result of electron mobility in a metallic conductor. The surface conductivity ( $\sigma^*_{\text{surface}}$ ) primarily depends upon the grain-surface morphology, and is also controlled by the pore fluid chemistry.

Electrical measurements are commonly used to determine the complex conductivity ( $\sigma^*$ ) of a material by measuring the conductivity magnitude ( $|\sigma|$ ) and phase shift ( $\phi$ ) of a sample relative to a reference resistor. These measurements are related to an in-phase energy loss term (conduction) represented by the real conductivity ( $\sigma'$ ) and an out-of-phase energy storage term (polarization) represented by the imaginary conductivity ( $\sigma''$ ) as follows,

$$|\sigma| = \sqrt{(\sigma')^2 + (\sigma'')^2} \quad (1),$$

$$\phi = \tan^{-1} \left( \sigma'' / \sigma' \right) \quad (2).$$

Therefore, the real and imaginary components are related to the phase as follows,

$$\sigma' = |\sigma| \cos \phi \quad (3),$$

$$\sigma'' = |\sigma| \sin \phi \quad (4).$$

The electrolytic and surface conductivity are often simply assumed to add in parallel for a porous medium (Waxman and Smits 1968). In this case, the real and imaginary parts of the

complex electrical conductivity ( $\sigma^*$ ) can be expressed as a function of the fluid conductivity ( $\sigma_w$ ) and the surface conductivity ( $\sigma^*_{\text{surface}}$ ) by :

$$\sigma' = \frac{1}{F} \sigma_w + \sigma'_{\text{surface}} \quad (5),$$

$$\sigma'' = \sigma''_{\text{surface}} \quad (6),$$

where F is the electrical formation factor (discussed further below), and single and double scripts represent real and imaginary part of the conductivity, respectively. Note that when surface conductivity is small,

$$|\sigma| \cong \sigma' \cong \frac{1}{F} \sigma_w \quad (7).$$

### 3. MATERIALS AND METHODS

#### 3.1. Preparation of ethanol-water and ethanol-salt solution mixtures

Pure ethanol (ethyl alcohol 200 proof, absolute ACS/USP grade, 99.98 % assay v/v) was used in this experiment. We prepared EtOH-water mixtures (0 to 0.97 v/v EtOH) by adding the desired volumes of pure EtOH and tap water in a volumetric flask and stirring at room temperature ( $26.0 \pm 0.5$  °C). Ethanol-salt solution mixtures (0 to 0.99 v/v EtOH) were prepared the same way. The salt solution, a Bushnell Haas Broth, was initially prepared in deionized water and comprised 0.81 mM of  $\text{MgSO}_4 \cdot 7\text{H}_2\text{O}$ , 0.14 mM of  $\text{CaCl}_2 \cdot 2\text{H}_2\text{O}$ , 7.35 mM of  $\text{KH}_2\text{PO}_4$ , 5.74 mM of  $\text{K}_2\text{HPO}_4$ , 12.44 mM of  $\text{NH}_4\text{NO}_3$  and 0.18mM of  $\text{FeCl}_3 \cdot 6\text{H}_2\text{O}$ . This salt solution is commonly used to examine microorganisms capable of degrading fuels and it can also be expected to serve as a surrogate for potentially mineralized groundwater where large spills of EtOH may occur.

Prepared salt solutions were sterilized by autoclaving at 121 °C for 30 minutes to prevent microbial growth of airborne bacteria that may be able to degrade EtOH and afterwards kept enclosed at ambient air and allowed to reach room temperature before being mixed with

ethanol in a volumetric flask. The solution was cooled down to room temperature to prevent EtOH volatilization during the mixture.

### 3.2. Conductivity measurements

We performed conductivity measurements for water, salt solution, EtOH-water and EtOH-salt solution mixtures using both a conductivity probe (Orion 013010A Thermo Electron Corporation) to measure  $\sigma_w$  and a four electrode electrical technique to measure complex conductivity ( $\sigma^*$ ). As pure EtOH is highly resistive, neither method could be used to measure conductivity of EtOH directly. The  $|\sigma|$  of EtOH-water mixtures varied dramatically but followed a second order polynomial function ( $R^2 \approx 1$ ) at EtOH > 90% v/v. The conductivity of pure EtOH was estimated by extrapolation based on the second order polynomial function of  $|\sigma|$  of the mixture as a function of EtOH concentration, from 90% to 97% EtOH v/v.

We directly measured fluid conductivity of the mixtures by inserting a probe in a sufficient volume of the fluid that was transferred into a clean beaker. Prior to each set of measurements, the probe was calibrated in a standard conductivity solution. The probe was rinsed with deionized water and wiped with task tissues after every single measurement. The electrical measurement used a four-electrode configuration, utilizing two electrodes as current injection and two additional electrodes to record the resulting potential difference. These measurements were performed between 1-1000 Hz using a two-channel dynamic signal analyzer (DSA) (NI-4461) on a flow through column (inner diameter=4.0c m, length= 17.3 cm) (Slater and Lesmes, 2002). Figure 1 shows a schematic of the column, including the location of two coiled Ag-AgCl current electrodes at each end and two Ag-AgCl potential electrodes (4.3 cm apart) along the side. Unlike the probe, the electrical method determines the complex conductivity of a porous material, and also allows measurements on a much

larger volume than the probe. In the case of solution mixtures only, the probe and electrical measurements should be equal (assuming homogeneous mixing of ethanol and water).

For measurements in the presence of a sand matrix, the column was dry-packed with Ottawa Sand ( $\text{SiO}_2 > 99\%$ , specific gravity= 2.65,  $d_{50}= 0.5\text{mm}$ ), with gentle tapping applied to minimize variations in the amount of compaction along the column.

### **3.3. Determination of the electrical formation factor**

The electrical formation factor (F) is defined as the ratio of the conductivity of a water-saturated porous medium to the conductivity of the water (Kobr et al, 2005). We determined F of the sand samples from the slope of the real conductivity ( $\sigma'$ ) at 1 Hz versus the fluid conductivity ( $\sigma_w$ ) (Figure 2) as per equation (5) (See for review Lesmes and Friedman, 2005).

### **3.4 Application of a mixing model**

The Lichtenecker-Rother (L-R) model, an effective medium theory, follows the symmetric Bruggeman rule that symmetric electromagnetic interactions occur among the components of a geomaterial (Cosenza et al., 2009). Such models offer a semi-analytical approach to examine a conceptual elementary volume of a geomaterial in terms of its constituent components. Effective medium theories are generally conceptualized on a simple cell containing a sub-spherical solid grain such as quartz sand embedded into a surrounding volume of fluid such as water. Commonly used in soil physics, they are valuable for characterizing the relationships between electromagnetic properties and hydrological variables (see Cosenza et al., 2009 for a review).

When ethanol is introduced into water, an arrangement of water molecules occurs as a result of attractive forces between the two components so that multi-hydration layers form around EtOH molecules (Frank and Wen, 1957; Parke and Birch, 1999). Therefore, like a solid grain of sand in water, an EtOH molecule can be seen as being embedded in many water molecules.

We applied a simple L-R model (Zakri et al, 1998; Cosenza et al., 2009) to our experimental data. We used the conductivity magnitude  $|\sigma|$  measured with the DSA as input data, although the same results would be obtained using real conductivity ( $\sigma'$ ) (e.g. Eq. 7). Assuming a negligible surface conduction in a two-phase mixture, this model is given by,

$$|\sigma|^\alpha = (1 - n)\sigma_2^\alpha + n\sigma_1^\alpha \quad (8),$$

where  $\sigma_1$  is the conductivity of water (236.34  $\mu\text{S}/\text{cm}$ ) or the salt solution (3633.60  $\mu\text{S}/\text{cm}$ ),  $\sigma_2$  is the conductivity of EtOH (0.252  $\mu\text{S}/\text{cm}$ ),  $n$  is the relative volume concentration of the water phase or salt-solution phase ( $0 \leq n \leq 1$ ) and  $\alpha$  is a fitting parameter ( $0 \leq \alpha \leq 1$ ). All parameters were known except  $\alpha$ , which was estimated from a least squares regression of the above models against the experimental data.

To account for the presence of the sand matrix in the case of an EtOH-salt solution in a sand matrix, the data were fit to the following adjusted model:

$$|\sigma|^\alpha = \frac{1}{F} [(1 - n)\sigma_2^\alpha + n\sigma_1^\alpha] \quad (9),$$

where  $F$  (6.62) is the electrical formation factor.

#### 4. RESULTS

The results of this experiment are summarized in Figures 3 to 5. Figure 3 shows a clear decrease in measured conductivity magnitude ( $|\sigma|$ ) for the three experimental treatments (EtOH-water mixture, EtOH-salt solution mixture, and EtOH-salt solution mixture in sand matrix) with increasing EtOH concentration. The decrease in  $|\sigma|$  shows a similar trend for all three experimental treatments. At very high EtOH concentration ( $\geq 0.70$  v/v), the drop in  $|\sigma|$  of the mixtures becomes much steeper.

The comparison between the experimental and modeled  $|\sigma|$  data for EtOH-water mixtures (0-0.97 v/v EtOH) and EtOH-salt solution mixtures (0-0.99 v/v EtOH) with and without sand

matrix is shown in Figure 4. The fitting parameter ( $\alpha$ ), determined from the least-squares regression approach, is respectively,  $0.28 \pm 0.01$ ,  $0.33 \pm 0.01$  and  $0.37 \pm 0.01$  for EtOH -water mixtures, EtOH-salt solution mixtures and EtOH-salt solution mixtures in the sand matrix.

The model fits the experimental data at concentration  $\leq 0.4$  v/v EtOH, but it cannot fit the data recorded at  $\geq 0.4$  v/v EtOH. In all three cases, measured  $|\sigma|$  is greater than that predicted by the model at concentration  $\geq 0.4$  v/v EtOH.

Figure 5 shows the variation in the measured phase response for selected concentrations of EtOH mixed with either water or salt solution (with or without a sand matrix). In all cases, the phase responses are negligible ( $\sim 0.1$  mrad) for all the mixtures at the low frequency range ( $\leq 100$  Hz). The increase in phase response at  $\geq 100$  Hz likely in part results from instrumentation effects such as capacitive coupling associated with the wiring to potential electrodes. However, it may also reflect the existence of other polarization mechanisms becoming important at higher frequencies.

## 5. DISCUSSION

### 5.1. Electrical properties of ethanol-liquid mixtures

The decrease in  $|\sigma|$  shows a similar trend for all three media (EtOH-water mixture, EtOH-salt solution mixture with and without sand matrix) as EtOH concentration increases (Figure 3).

The initial conductivity values of the mixture components were  $236.34 \mu\text{S}/\text{cm}$  for water,  $3633.60 \mu\text{S}/\text{cm}$  for the salt solution and  $0.252 \mu\text{S}/\text{cm}$  (estimated) for pure EtOH. Our estimated conductivity of EtOH is comparable with that of  $0.554 \mu\text{S}/\text{cm}$  obtained in a previous study using a conductivity meter designed for very low conductivity measurement (Prego et al., 2000). Since pure EtOH is highly resistive, its addition to the mixtures reduces the mixture  $|\sigma|$ . However, an equal increment of EtOH does not result in a linear or an exponential decrease in  $|\sigma|$ , thus suggesting varied and complex intermolecular interactions

between the components of the mixtures as the ratio of EtOH to water or salt solution changed. Previous studies have shown that EtOH and water chemically interact (hydrogen bonding) to form a complex mixture (Franks and Ives, 1966; Parke and Birch, 1999, Atamas and Atamas, 2009).

That ethanol molecules have both a hydrophilic hydroxyl group favorable to hydrogen-bonding with water molecules and an alkyl chain conferring hydrophobic effects may shed light on the complexity and types of interactions involved in EtOH-water mixtures and their influence on the electrical conductivity observed here. Unlike dissolution, a kinetic process that is quantified by its rate, solvation (interaction of a solute with a solvent leading to a solution whereby the solute species is stabilized, IUPAC, 2006) could better explain the types of interaction and association occurring in EtOH-water mixtures. During this solvation process, different types of attractive forces are involved among water and EtOH molecules. The mobility of water molecules may have been affected as they are attracted and form multi-hydration layers around EtOH molecules.

The formation of immobilized water layers was documented previously for ion-solvent interaction in aqueous solutions (Frank and Wen, 1957) and inferred elsewhere for EtOH-water interaction (Parke and Birch, 1999). As a result, the ionic mobility of the solution could be affected. Bhat and Shetty (2011), observing a rapid decrease in limiting molar conductance of water containing sulfacetamide sodium following the addition of EtOH, suggested a reduction in solvated ionic mobility as a result of the formation of intermolecular hydrogen bonding. Therefore, a relation is inferred between the measured  $|\sigma|$  values and the solvation driven changes in the ionic mobility of EtOH-water and EtOH-salt solution. The steeper decrease in  $|\sigma|$  at very high EtOH concentration  $\geq 0.7$  v/v probably reflects limited availability of ions in the small volume proportion of water or salt solution in the mixtures. Measurements

performed directly on the EtOH-water and EtOH-salt solution mixtures using the conductivity meter (data not shown) were comparable to those with the electrical method, confirming the accuracy and precision of the electrical measurements.

## 5.2. Modeling of ethanol-liquid mixtures

The applied Lichtenecker-Rother (L-R) model yields similar results for both our estimated  $|\sigma|$  value for ethanol ( $0.252 \mu\text{S}/\text{cm}$ ) and the value of  $0.554 \mu\text{S}/\text{cm}$  of pure EtOH reported elsewhere (Prego et al, 2000). The model fits the  $|\sigma|$  data for EtOH concentration  $\leq 0.4$  v/v while deviations from the model are observed at higher EtOH concentration in the mixture (Figure 4). These findings likely result from the complexity and different types of interactions of EtOH and water molecules. Atamas and Atamas (2009) described three types of interactions occurring in water-ethanol mixtures: water-water interaction, EtOH-water interaction and EtOH-EtOH interaction (Figure 6).

As EtOH concentration increases, it can be seen (Figure 6) that the water-water energy interaction decreases while the EtOH-EtOH interaction increases. However, the water-EtOH energy interaction shows a multiphase profile curve with: a) a rapid increase up to  $\sim 0.4$  v/v EtOH, b) a relative plateau from  $\sim 0.4$  to  $0.7$  v/v EtOH and, c) a rapid decrease after  $\sim 0.7$  v/v EtOH. The fit of the L-R model with the experimental data at EtOH concentration  $\leq 0.4$  v/v is consistent with a strong water-EtOH interaction mainly through intercomponent hydrogen bonding formation. Although several forces can act simultaneously during the solvation process occurring in water-EtOH media, hydrogen bonding remains predominant in defining their association (Atamas and Atamas, 2009). As EtOH is introduced into water, a structural rearrangement of water molecules occurs such that EtOH and water are strongly attracted. As depicted in the modeled and the experimental curves (Figure 4), the log of  $|\sigma|$  is linearly related to EtOH concentration at  $\leq 0.4$  v/v. This trend can be explained by the fact

that the water-EtOH interaction is optimized and more influential than the water-water and EtOH-EtOH interactions. In that range, the modeled and experimental data fit because the applied L-R model assumes a symmetric interaction between the two components of the mixture. Note that EtOH is toxic to soil and aquifer microorganisms at concentration  $\geq 0.06$  v/v (Nelson et al, 2010), but its biodegradation can occur at lower concentration if sufficient nutrients, along with O<sub>2</sub> or other terminal electron acceptors are available. The biodegradation of EtOH may result in various byproducts including dissolved acetic and carbon acid that can lead to changes in fluid conductivity and, subsequently, in bulk conductivity. However, we did not observe visible contamination indicative of microbial activity and/or EtOH biodegradation.

Our results are therefore consistent with the rapid increase of water-EtOH energy interaction illustrated in Figure 6. Furthermore, they are in agreement with previous studies showing a minimum in the apparent specific volumes of EtOH in water at low EtOH concentrations ( $\sim 25$  % w/w) (Franks and Ives 1966, Parke and Birch, 1999), thus indicating a better packing efficiency between EtOH and water molecules due to strong intermolecular interactions. Our findings are also supported by previous observations on solution properties of EtOH in water such as the maximum in the sound velocity, the formation of a more compact hydration layer (minimum value of the isentropic compressibility coefficient) as a result of strong intercomponent hydrogen bonding formation, and the increased number of water molecules displaced by EtOH molecules (compressibility hydration numbers) at low EtOH concentrations (Parke and Birch, 1999). All of these parameters indicate the extent of high and predominant water-EtOH or EtOH-salt solution interactions in the mixtures.

The existence of hydrophobic effects, which start to occur at  $\sim 0.4 - 0.5$  v/v EtOH as suggested in Figure 6, could explain the observed deviation between the modeled and

experimental  $|\sigma|$  data at high EtOH concentrations. These effects may take place in water-EtOH mixtures as a result of the formation of linear chains or rings of self-associated EtOH molecules (Mizuno et al, 1995; Franks and Ives, 1966), which removes their hydrophobic parts from contact with water (Wiggins, 1997). Atamas and Atamas (2009) pointed out that the water-EtOH mixture forms an ideal solution at  $\sim 0.4$  v/v EtOH and follows Raoult's law, thus indicating an equilibrium state in the solution. At ethanol concentration  $\geq 0.4$  v/v, the solution structure has changed. The aforementioned predominant intercomponent hydrogen bonding at concentration  $\leq 0.4$  v/v EtOH is presumably weakened as EtOH-EtOH interaction increases over the point of equilibrium (Figure 6). Weaver et al. (2009) showed a gradual increase in hydrophobicity in EtOH-water-hydrocarbon system at  $\sim 0.4 \leq \text{EtOH} \leq 0.7$  v/v, followed by a complete phase separation into a predominantly aqueous-alcohol phase and a predominantly oil phase at  $\sim \text{EtOH} > 0.7$  v/v. As pure ethanol (ethyl alcohol 200 proof, absolute ACS/USP grade, 99.98 % assay v/v) (i.e. hydrocarbon content  $< 0.02$  % v/v) was used in our experiment, a phase separation with an oil phase is not plausible. Instead, in our binary EtOH-water system, it is most likely that the influence of hydrophobic effects becomes particularly important at very high EtOH concentration ( $> 0.70$  v/v) such that water or salt solution clusters (partial phase separation into EtOH and water or salts) could potentially occur. Similar observations of water cluster formation and enhancement of water-water interaction energy in the bulk of water-pyridine system were reported previously (Sinoti et al., 1996). Both the weakening of water-EtOH interaction and the formation of water and salt solution clusters could facilitate ionic mobility in the solution. Therefore, they could be responsible for observed higher experimental  $|\sigma|$  values in comparison with the modeled data. As the applied L-R model is based on the assumptions of symmetric interactions between the components of the mixtures, it cannot reflect such asymmetric changes occurring in the media

at high EtOH concentrations. Our observations herein are consistent with previous studies that reported an increase of water-water aggregation (Atamas and Atamas, 2009) and a decrease of water-EtOH molecules interacting by hydrogen bonding (Parke and Birch, 1999; Atamas and Atamas, 2009) at very high EtOH concentration in water-EtOH media.

Subsurface EtOH contamination can potentially vary from very low to high concentration. Previous studies have shown that EtOH transport in porous media resulted in high EtOH concentration, with ethanol trapped in the unsaturated zone and slowly diffusing into the shallow groundwater (Cápiro et al., 2007; Stafford and Rizzey, 2011; Freitas and Barker, 2011b; Freitas and Barker, 2011c). In such situations, EtOH concentration may potentially exceed 0.4 v/v in the unsaturated zone, the concentration beyond which the applied L-R model becomes invalid based on our results. However, owing to high EtOH-water miscibility, it is likely that EtOH dilution occurs as it partitions into a sufficient volume of pore water in the unsaturated zone and the capillary fringe. Furthermore, fluctuations in the water table may potentially increase the mixing of EtOH with the saturated and unsaturated zone pore water, such that EtOH may be significantly diluted near the source zone.

### **5.3. Interfacial polarization of ethanol-liquid mixtures**

The electrical  $|\sigma|$  measurements show no evidence of interfacial polarization effects at the EtOH-liquid interfaces (Figure 5). As an electric current is applied to the EtOH-liquid mixture, the presence of an interface between EtOH and water could conceivably result in an electrical double layer (EDL). The migration and redistribution of ions in the EDL could result in an electrochemical polarization effect as charges tend to built up at the interface. However, if such an EDL does form, the signal associated with its polarization is clearly too weak to be detected with conventional electrical methods as our measurements of phase responses are negligible ( $\leq 0.1$  mrad) in all EtOH-liquid mixtures at the low frequency

measurements ( $\leq 100$  Hz) (Figure 5). At frequencies  $\geq 100$ Hz, the Maxwell-Wagner polarization (MW) could potentially occur at the interface (e.g. Leroy et al., 2008). However, we mainly attribute the small phase response observed (0.2 - 0.5 mrad) in the frequency range  $\geq 100$ Hz as being instrumentation effects associated with the wiring to potential electrodes.

#### **5.4. Influence of sand matrix on the polarization effects**

We also observed no evidence of substantial interfacial polarization effects at the EtOH/liquid/mineral interface. Similar to the discussion above, the double layer polarization and the MW polarization could potentially exist at the ethanol/liquid/mineral interface. However, the phase responses remain very small (0.2-0.5 mrad) over the measured frequency range. Therefore, our results show no clear evidence of changes in the polarization effects due to the presence of the sand matrix. Furthermore, the measurements in the sand matrix confirmed that the  $|\sigma|$  results could simply be scaled by the formation factor (F) as indicated by the comparable fitting parameter ( $\alpha = 0.33 \pm 0.01$  and  $\alpha = 0.37 \pm 0.01$ , respectively) obtained from the conductivity model for measurements performed with and without sand matrix (Figure 4). We recognize that this experiment was conducted in a simple sand matrix while more complex environmental conditions may prevail in the field. As different environmental settings may influence substantially the polarization effects, further investigations need to be conducted to establish the potential effects of EtOH in more complex matrices (e.g. in the presence of clays).

## **6. CONCLUSIONS**

Our experiment has demonstrated the sensitivity of electrical conductivity measurements to the interactions occurring in EtOH-liquid mixtures as EtOH concentration is varied. The measured  $|\sigma|$  values were related to the changes in solution properties, which may reflect

solvation driven changes in ionic mobility. We also demonstrated that a simple mixing model can be combined with electrical data to reasonably estimate EtOH concentration at  $\leq 0.4$  v/v EtOH in the mixture. The model could not fit the experimental data at  $\geq 0.4$  v/v EtOH presumably due to subtle asymmetric changes in water-EtOH mixtures associated with important hydrophobic effects of EtOH molecules. Our results highlight the potential for using non-invasive and cost-efficient geophysical techniques to detect and monitor EtOH concentrations in the subsurface. Such tools may ultimately serve to assess EtOH-contaminated sites and aid in the decision-making process regarding appropriate remediation strategies.

#### **ACKNOWLEDGEMENTS**

The United States Environmental Protection Agency through its Office of Research and Development partially funded and collaborated in the research described here under contract # EP10D000751 to Yves Robert Personna. The manuscript has been subjected to EPA review and approved for publication.

We thank the editor and an anonymous reviewer for their constructive comments that helped improve the manuscript. Jacob Gibbs (USGS, Trenton) provided valuable review comments on an earlier version of this manuscript.

The use of brand names is for identification purposes only and does not constitute endorsement by the U.S. Government.

#### **REFERENCES**

Atamas, N.A., Atamas, A.A., 2009. The Investigations of Water-ethanol Mixture by Monte Carlo Method. World Academy of Science, Engineering and Technology, 55, 1-4.

- Bhat, J.I., Shetty, M.K., 2011. Evaluation of limiting molar conductance, Walden product, association constant and thermodynamic properties of sulfacetamide sodium in water+EtOH mixtures: *Journal of Molecular Liquids*, 160, no. 3, p. 140-143, doi: 10.1016/j.molliq.2011.03.005.
- Cápiro, N.L., Da Silva, M.L.B., Stafford, B.P., Rixey, W.G., Alvarez, P.J.J., 2008. Microbial community response to a release of neat ethanol onto residual hydrocarbons in a pilot-scale aquifer tank: *Environmental microbiology*, v. 10, no. 9, p. 2236-44, doi: 10.1111/j.1462-2920.2008.01645.x.
- Cápiro, N. L., Stafford, B. P., Rixey, W., Bedient, G. P.B., Alvarez, P.J.J., 2007. Fuel-grade ethanol transport and impacts to groundwater in a pilot-scale aquifer tank. *Water Research*, v. 41, no 3, p. 656-664, doi:10.1016/j.watres.2006.09.024.
- Corseuil, H.X., Kaipper, B.I. A, Fernandes, M., 2004. Cosolvency effect in subsurface systems contaminated with petroleum hydrocarbons and ethanol: *Water research*, v. 38, no. 6, p. 1449-56, doi: 10.1016/j.watres.2003.12.015.
- Corseuil, H.X., Hunt, C.S., Ferreira dos Santos, R.C., Alvarez, P.J.J., 1998. The influence of the gasoline oxygenate ethanol on aerobic and anaerobic BTX biodegradation: *Water Research*, v. 32, no. 7, p. 2065-2072, doi: 10.1016/S0043-1354(97)00438-7.
- Cosenza, P., Ghorbani, A., Camerlynck, C., Rejiba, F., Guérin, R., Tabbagh, A., 2009. Effective medium theories for modelling the relationships between electromagnetic properties and hydrological variables in geomaterials: a review: *Near Surface Geophysics*, p. 563-578, doi: 10.3997/1873-0604.2009009.

- Da Silva, M.L.B., Alvarez, P.J.J., 2002. Effects of Ethanol versus MTBE on Benzene, Toluene, Ethylbenzene, and Xylene Natural Attenuation in Aquifer Columns: Journal of Environmental Engineering, v. 128, no. 9, p. 862, doi: 10.1061/(ASCE)0733-9372(2002)128:9(862).
- EPA, 2011. Four dimensional geophysical measurements of a controlled ethanol release in Ottawa sand. APM 253. Glaser, D. R., Werkema, D. D., Henderson, R.D., Johnson, T., Versteeg, R. J., Lane, J. W.

- Frank, H.S., Wen, W.-Y., 1957. Ion-solvent interaction. Structural aspects of ion-solvent interaction in aqueous solutions: a suggested picture of water structure: *Discussions of the Faraday Society*, v. 24, p. 133, doi: 10.1039/df9572400133.
- Franks, F., Ives, D.J.G., 1966. The structural properties of alcohol-water mixtures: *Quarterly Reviews, Chemical Society*, v. 20, no. 1, p. 1, doi: 10.1039/qr9662000001
- Freitas, J.G., Mocanu, M.T., Zoby, J.L.G., Molson, J.W., Barker, J.F., 2011a. Migration and fate of ethanol-enhanced gasoline in groundwater: A modeling analysis of a field experiment: *Journal of contaminant hydrology*, v. 119, no. 1-4, p. 25-43, doi: 10.1016/j.jconhyd.2010.08.007.
- Freitas, J.G., Barker, J.F., 2011b. Oxygenated gasoline release in the unsaturated zone - Part 1: Source zone behavior: *Journal of contaminant hydrology*, v. 126, no. 3-4, p. 153-66, doi: 10.1016/j.jconhyd.2011.07.003.
- Freitas, J.G., Barker, J.F., 2011c. Monitoring Lateral Transport of Ethanol and Dissolved Gasoline Compounds in the Capillary Fringe: *Ground Water Monitoring & Remediation*, vol. 31, no. 3, p. 95-102, doi: 10.1111/j1745.
- Freitas, J.G., Fletcher, B., Aravena, R., and Barker, J.F., 2010. Methane production and isotopic fingerprinting in ethanol fuel contaminated sites.: *Ground water*, v. 48, no. 6, p. 844-57, doi: 10.1111/j.1745-6584.2009.00665.
- Gomez, D.E., Alvarez, P.J.J., 2010. Comparing the effects of various fuel alcohols on the natural attenuation of benzene plumes using a general substrate interaction model.: *Journal of contaminant hydrology*, v. 113, no. 1-4, p. 66-76, doi: 10.1016/j.jconhyd.2010.02.002.

- Gomez, D.E., Alvarez, P.J.J., 2009. Modeling the natural attenuation of benzene in groundwater impacted by ethanol-blended fuels: Effect of ethanol content on the lifespan and maximum length of benzene plumes: *Water Resources Research*, v. 45, no. 3, p. 1-9, doi: 10.1029/2008WR007159.
- Henderson, R.D., Werkema, D.D. Jr., Horton, R.J., Lane, J.W. Jr., 2009. Broadband electrical signatures of water-ethanol solutions in Ottawa Sand [abs.]: *EOS Transactions, American Geophysical Union*, 90 (52), Fall Meeting Supplement, abstract NS23A-1133
- Ingram, L.O., 1990. Ethanol tolerance in bacteria. *Crit Rev Biotechnol.*, 9 (4).
- IUPAC, 2006. *Compendium of Chemical Terminology*, 2nd ed. (the "Gold Book", 1997).  
Web. <<http://old.iupac.org/publications/compendium/S.html>>.
- Leroy, P., Revil, A., Kemna, A., Cosenza, P., Ghorbani, A., 2008. Complex conductivity of water-saturated packs of glass beads.: *Journal of colloid and interface science*, v. 321, no. 1, p. 103-17, doi: 10.1016/j.jcis.2007.12.031.
- Lesmes, D.P., Friedman, S.P., 2005. Relationships between the electrical and hydrogeological properties of rocks and Soils. In: Rubin Y, Hubbard S (eds), *Hydrogeophysics*. Springer, The Netherlands, pp 87–128.
- Ma, J., Xiu, Z., Monier, A.L., Mamonkina, I., Zhang, Y., He, Y., Stafford, B.P., Rixey, W.G., Alvarez, P.J.J., 2011. Aesthetic Groundwater Quality Impacts from a Continuous Pilot-Scale Release of an Ethanol Blend: *Ground Water Monitoring & Remediation*, v.31, no. 3, p. 47-54, doi: 10.1111/j1745.
- Mackay, D.M., De Siewes, N.R., Einarson, M.D., Feris, K.P., Pappas, A. A., Wood, I. A., Jacobson, L., Justice, L.G., Noske, M.N., Scow, K.M., Wilson, J.T., 2006. Impact of

ethanol on the natural attenuation of benzene, toluene, and o-xylene in a normally sulfate-reducing aquifer: *Environmental science & technology*, v. 40, no. 19, p. 6123-30.

McDowell, C.J., Buscheck, T., Powers, S.E., 2003. Behavior of Gasoline Pools Following a Denatured Ethanol Spill: *Ground Water*, v.41, no.6, p. 746–757, DOI: 10.1111/j.1745-6584.2003.tb02416.x.

Mcnaughton, C.H., Mosquera, J.D., Endres, A.L., Freitas, J.G., 2009. Monitoring of Sequential Gasoline-Ethanol Releases using High Frequency Ground Penetrating Radar: *IEEE*, p. 1-6.

Mizuno, K., Miyashita, Y., Shindo, Y., Ogawa, H., 1995. NMR and FT-IR Studies of Hydrogen Bonds in Ethanol-Water Mixtures: *The Journal of Physical Chemistry*, v. 99, no. 10, p. 3225-3228, doi: 10.1021/j100010a037.

Nelson, D.K., Lapara, T.M., Novak, P.J., 2010. Effects of ethanol-based fuel contamination: microbial community changes, production of regulated compounds, and methane generation: *Environmental science & technology*, v. 44, no. 12, p. 4525-30, doi: 10.1021/es903940q.

Parke, S. A., Birch, G.G., 1999. Solution properties of ethanol in water: *Food Chemistry*, v. 67, no. 3, p. 241-246, doi: 10.1016/S0308-8146(99)00124-7.

Petek, A., Pečar, D., Doleček, V., 2001. Volumetric Properties of Ethanol-Water Mixtures under High Pressure. *Acta Chim. Solv.*, 48, 317-324.

Petong, P., Pottel, R., Kaatze, U., 2000. Water-Ethanol Mixtures at Different Compositions and Temperatures. A Dielectric Relaxation Study: *The Journal of Physical Chemistry A*, v. 104, no. 32, p. 7420-7428, doi: 10.1021/jp001393r.

- Powers, S.E., Rice, D.W., Dooher, B., Alvarez, P.J.J., 2001a. Will Ethanol-Blended Gasoline Affect Groundwater Quality? *Environmental Science and Technology*, v. 35, no. 1, p. 24A-29A.
- Powers, S.E., Hunt, C., Heermann, S., Corseuil, H., Rice, D., Alvarez, P., 2001b. The Transport and Fate of Ethanol and BTEX in Groundwater Contaminated by Gasohol: *Critical Reviews in Environmental Science and Technology*, v. 31, no. 1, p. 79-123, doi: 10.1080/20016491089181.
- Prego, M., Cabeza, O., Carballo, E., Franjo, C.F., Jimenez, E., 2000. Measurement and interpretation of the electrical conductivity of 1-alcohols from 273 K to 333 K: *Journal of Molecular Liquids*, v. 89, no. 1-3, p. 233-238, doi: 10.1016/S0167-7322(00)90016-3.
- Ruiz-Aguilar, G.M.L., O'Reilly, K., Alvarez, P.J.J. 2003. A Comparison of Benzene and Toluene Plume Lengths for Sites Contaminated with Regular vs. Ethanol-Amended Gasoline: *Ground Water Monitoring & Remediation*, v.23, no.1, p.48-53.
- Sinoti, A.L.P., Politi, J.R.D.S., Freitas, L.C.G., 1996. Monte Carlo Simulation of Water-Pyridine Mixtures: *J. Braz. Chem. Soc.*, v.7, no. 2, p.133-141.
- Slater, L., Lesmes, D. L. 2002. Electrical-hydraulic relationships observed for unconsolidated sediments: *Water Resources Research*, v. 38, no. 10, p. 1-13, doi: 10.1029/2001WR001075.
- Spalding, R.F., Toso, M.A., Exner, M.E., Hattan, G., Higgins, T.M., Sekely, A.C., Jensen, S.D., 2011. Long-Term Groundwater Monitoring Results at Large, Sudden Denatured Ethanol Releases: *Ground Water Monitoring & Remediation*, v.31, no. 3, p. 69-81, doi: 10.1111/j1745.

- Stafford, B.P., Rixey, W.G., 2011. Distribution of Fuel-Grade Ethanol near a Dynamic Water Table: *Ground Water Monitoring & Remediation*, v.31, no. 3, p. 55-60, doi: 10.1111/j1745.
- Stafford, B.P., Cápiro, N.L., Alvarez, P. J.J., Rixey, W. G., 2009. Pore Water Characteristics Following a Release of Neat Ethanol onto Pre-existing NAPL. *Ground Water Monitoring & Remediation*, v. 29, no.3, p. 93–104.
- “Weaver, J.M., Shaggs, S.A., Spidle, D.L., Stone, G.C., 2009. Composition and Behavior of Fuel Ethanol. EPA/600/R-09/037; p.1-69”.
- Wiggins, P.M., 1997. Hydrophobic hydration, hydrophobic forces and protein folding. *Physica A* 238, 113- 128.
- Zakri, T., Laurent, J.-P., Vauclin, M., 1998. Theoretical evidence for 'Lichtenecker's mixture formulae' based on the effective medium theory: *Journal of Physics D: Applied Physics*, v. 31, no. 13, p. 1589-1594, doi: 10.1088/0022-3727/31/13/013

## FIGURE CAPTIONS

Figure 1: Schematic of experimental setup showing dynamic signal analyzer (NI 4461) with analog input and output, reference resistance ( $R_{ref}$ ), location of preamplifier (AD 620), column configuration with two coiled Ag-AgCl current electrodes ( $C_1$  &  $C_2$ ) and two Ag-AgCl potential electrodes ( $P_1$  &  $P_2$ ), inflow and outflow valves and flow direction.

Figure 2: Plot of real conductivity ( $\sigma'$ ) at 1Hz versus fluid conductivity ( $\sigma_w$ ): dark squares are experimental data while the dark line is the linear regression fit of the data; the equation of this regression is shown as well as the  $R^2$  value. The formation factor ( $F$ ) and  $\sigma'_{surface}$  are 6.62 and 3.90  $\mu\text{S}/\text{cm}$ , respectively.

Figure 3: Variation in measured conductivity magnitude  $|\sigma|$  of ethanol-water mixture (plus sign), ethanol-salt solution mixture (dark circles) and ethanol-salt solution mixture in sand matrix (open circles) at increased ethanol concentration.

Figure 4: Comparison of measured conductivity magnitude ( $|\sigma|$ ) between the Lichtenecker-Rother modeled data (black line for our estimated pure ethanol electrical conductivity of 0.252  $\mu\text{S}/\text{cm}$  and blue line for the value of 0.554  $\mu\text{S}/\text{cm}$  reported by Prego et al., 2000) and a) ethanol-water mixture experimental data (plus sign), b) ethanol-salt solution mixture experimental data (dark circles), and c) ethanol-salt solution mixture in sand matrix experimental data (open circles). The fitting parameters ( $\alpha$  and  $\alpha'$  for ethanol conductivity of 0.252 and 0.554  $\mu\text{S}/\text{cm}$ , respectively) determined from the least-squares regression approach, are shown.

Figure 5: Variation in phase ( $\phi$ ) for selected ethanol concentration, a) ethanol-water mixture, b) ethanol-salt solution mixture and c) ethanol-salt solution mixture in sand matrix

Figure 6: Types and complexity of water-ethanol mixtures interactions (adapted from Atamas and Atamas, 2009)

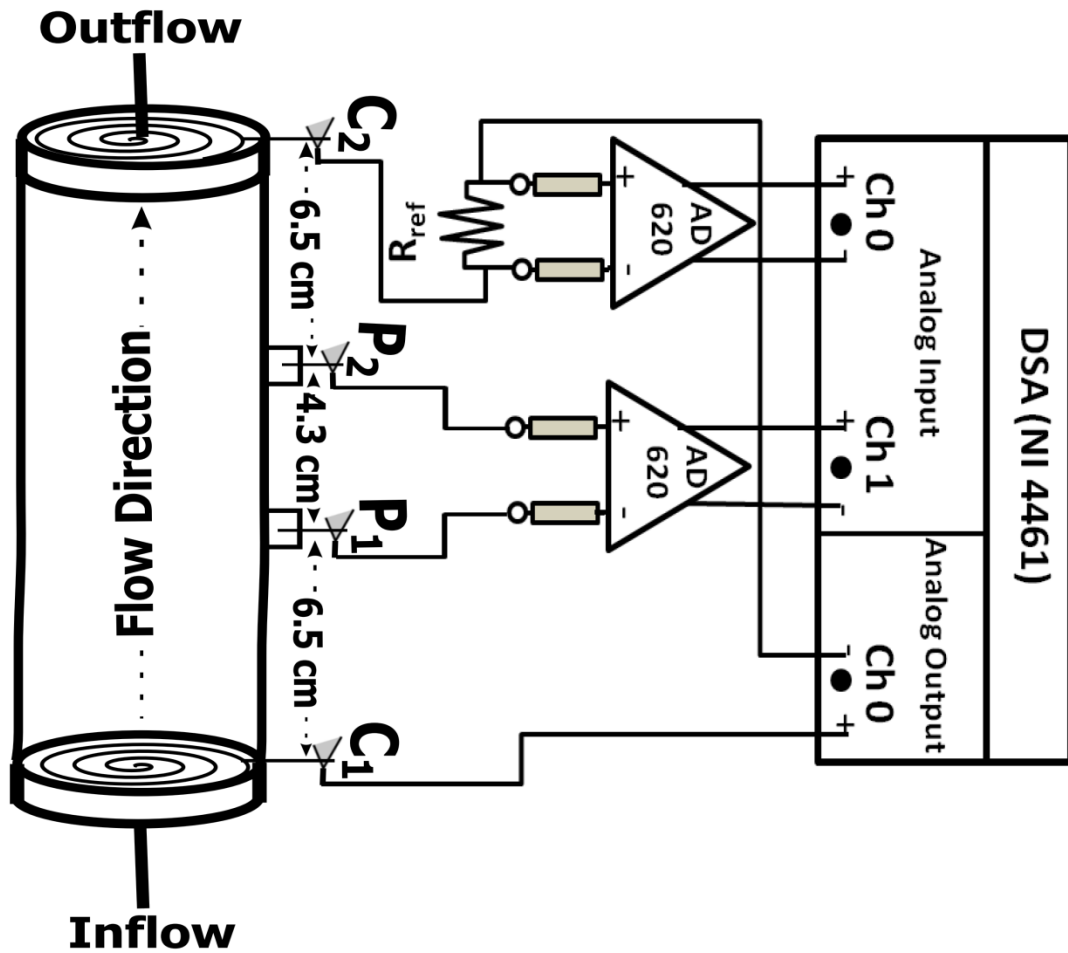


Figure 1: Schematic of experimental setup showing dynamic signal analyzer (NI 4461) with analog input and output, reference resistance ( $R_{ref}$ ), location of preamplifier (AD 620), column configuration with two coiled Ag-AgCl current electrodes ( $C_1$  &  $C_2$ ) and two Ag-AgCl potential electrodes ( $P_1$  &  $P_2$ ), inflow and outflow valves and flow direction.

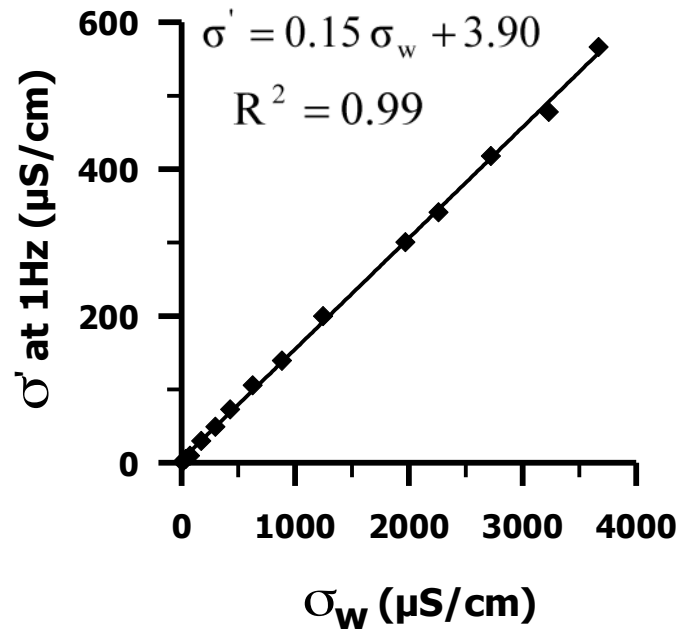


Figure 2: Plot of real conductivity ( $\sigma'$ ) at 1Hz versus fluid conductivity ( $\sigma_w$ ): dark squares are experimental data while the dark line is the linear regression fit of the data; the equation of this regression is shown as well as the  $R^2$  value. The formation factor (F) and  $\sigma'_{\text{surface}}$  are 6.62 and 3.90  $\mu\text{S/cm}$ , respectively.

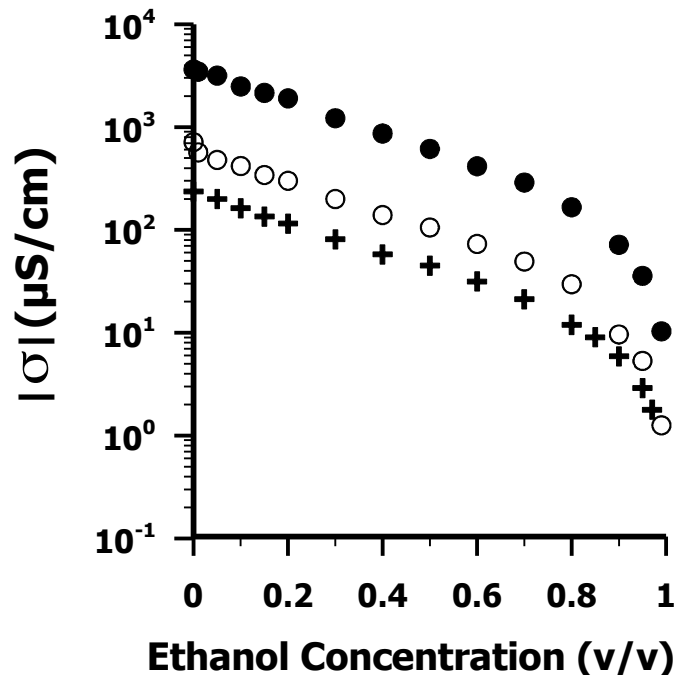


Figure 3: Variation in measured conductivity magnitude  $|\sigma|$  of ethanol-water mixture (plus sign), ethanol-salt solution mixture (dark circles) and ethanol-salt solution mixture in sand matrix (open circles) at increased ethanol concentration.

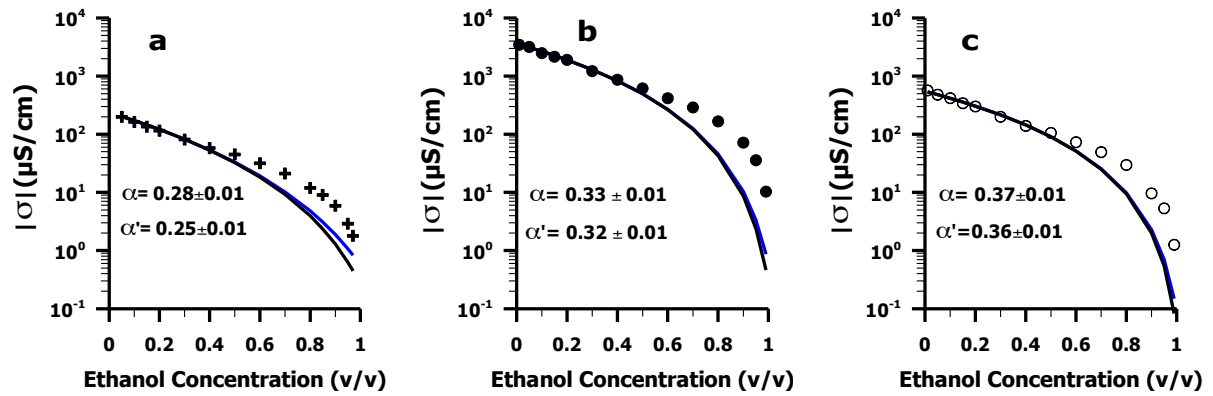


Figure 4: Comparison of measured conductivity magnitude ( $|\sigma|$ ) between the Lichtenecker-Rother modeled data (black line for our estimated pure ethanol electrical conductivity of  $0.252 \mu\text{S/cm}$  and blue line for the value of  $0.554 \mu\text{S/cm}$  reported by Prego et al., 2000) and a) ethanol-water mixture experimental data (plus sign), b) ethanol-salt solution mixture experimental data (dark circles), and c) ethanol-salt solution mixture in sand matrix experimental data (open circles). The fitting parameters ( $\alpha$  and  $\alpha'$  for ethanol conductivity of  $0.252$  and  $0.554 \mu\text{S/cm}$ , respectively), determined from the least-squares regression approach, are shown.

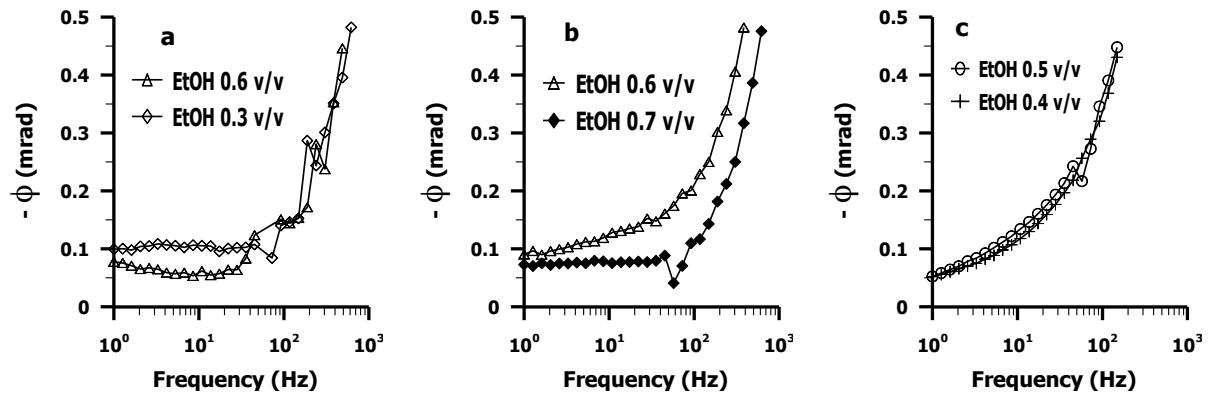


Figure 5: Variation in phase ( $\phi$ ) for selected ethanol concentration, a) ethanol-water mixture, b) ethanol-salt solution mixture and c) ethanol-salt solution mixture in sand matrix

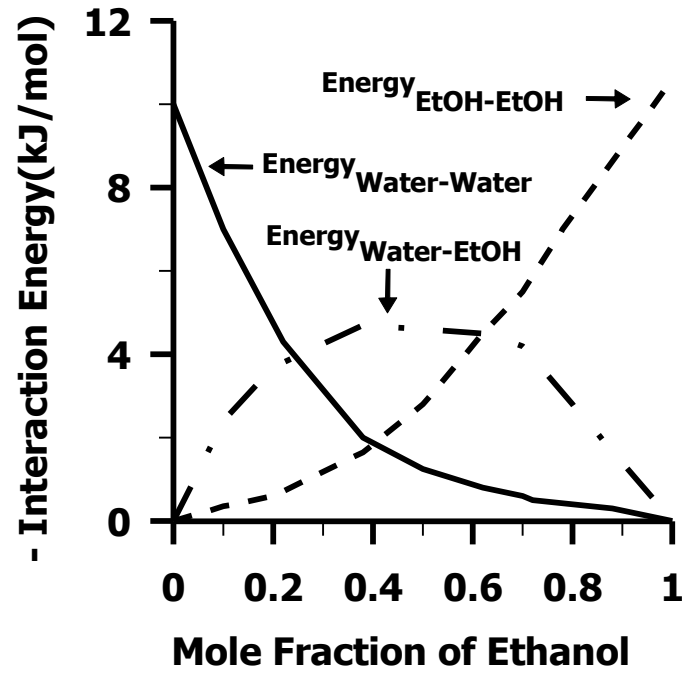


Figure 6: Types and complexity of water-ethanol mixtures interactions (adapted from Atamas and Atamas, 2009)